Phase Based Spatial Identification of UHF RFID Tags

Pavel V. Nikitin, Rene Martinez, Shashi Ramamurthy, Hunter Leland, Gary Spiess, and K. V. S. Rao
Intermec Technologies Corporation
6001 36th Ave W, Everett, WA, 98203, USA
{pavel.nikitin, rene.martinez, shashi.ramamurthy, hunter.leland, gary.spiess, kvs.rao}@intermec.com

***Abstract*— In this paper, we give an overview of spatial identification (determining position and velocity) of modulated backscatter UHF RFID tags using RF phase information. We describe three main techniques based on PDOA (Phase Difference of Arrival): TD (Time Domain), FD (Frequency Domain), and SD (Spatial Domain). The techniques are illustrated with modeling and simulation example in free space and in presence of multipath using a multi-ray channel model for amplitude and phase of the received tag signal in deterministic environment. We also present and discuss the experiments performed in a real RFID warehouse portal environment.**

I. INTRODUCTION

Real time locating systems (RTLS, also known as location tracking, location sensing, location positioning, localization, etc.) have always been a subject of strong interest in wireless industry. Classical wireless approaches to positioning employ triangulation using received signal strength indicator (RSSI) as in cell phones and time difference of arrival (TDOA) as in GPS. Good overviews of wireless positioning techniques can be found in [1-5]. Source localization has also been a subject of interest and research in acoustic [6-7] and underwater [8-9] communications, where mechanical instead of electromagnetic waves are used [10].

Some of the classical wireless positioning approaches are in general applicable to RFID as discussed in [11-12]. However, modulated backscatter UHF RFID is a very short range narrowband technology, with typical tag read range on the order of 10-20 ft (for passive tags) and maximum available bandwidth of 26 MHz (unlicensed ISM band 902-928 MHz in US). Because the roundtrip signal delay is on the order of a few tens of nanoseconds and the bandwidth is narrow, RFID readers and tags can not operate in short pulse mode required for TDOA distance determination. Thus common tag localization techniques use either read/no read criteria (with tags as markers [13-14], readers as markers [15-16], or with adaptive power control on the reader side [17-18]) or use RSSI (Received Signal Strength Indicator) information from the tag signal [19-21]. However, RSSI is usually severely affected by the propagation environment, the tagged object properties, etc. and cannot be universally approximated with free space or similar distance-dependent path loss model. Besides, absolute calibration of RSSI is rather difficult. Finally, the tag backscatter loss varies with the power incident on the tag (which itself varies with the tag location) because input impedance of RFID tag IC is power dependent.

Fortunately, RFID readers perform fully coherent detection and recover the baseband phase of the coherently demodulated tag signal even though this information may not be visible or made available to the users. Thus, tag phase information is becoming increasingly important for such advanced RFID applications as *spatial identification* (determining tag position and velocity). We prefer to use this term because it suggests that one can not only obtain tag data information but also obtain additional information about tag spatial characteristics.

Phase of the tag signal depends both on the propagation channel and the modulating properties of the tag, which can be both frequency- and power-dependent. However, all these factors are additive (rather than multiplicative) and in many cases can be calibrated out if phase difference of arrival (PDOA) is used. In this paper, we present an overview of phase based spatial identification of RFID tags. Some of the equations and terminology previously appeared in the cited references, but never were summarized together in application to modulated backscatter UHF RFID. To illustrate all three main techniques based on phase difference of arrival (TD-PDOA, FD-PDOA, and SD-PDOA), we show simulation results for a simple modeling example of a tag moving by a pair of reader antennas in the presence of multipath. We also experimentally demonstrate TD-PDOA technique using data collected on real Gen2 tags using our custom reader capable of accurately measuring RSSI and phase of the tag signal at different frequency channels. The data was collected in one of the most practical RFID environments – a warehouse portal.

II. TAG PHASE

Most RFID readers perform fully coherent detection and can measure both the power and the phase of the tag signal. Tag phase can be best explained in phasor space (I-Q plane of the received baseband voltage) shown in Fig. 1. The complex demodulated voltage at the reader receiver at any given moment of time can be written as sum of three components:

$$\vec{V} = \vec{V}_{leakage} + \vec{V}_{clutter} + \vec{V}_{tag}^{\,i}\ , \qquad (1)$$

where $\vec{V}_{leakage}$ is the voltage due to the reader transmit-receive leakage (including reflection from the mismatched reader antenna), $\vec{V}_{clutter}$ is the voltage due to the scatter from the static environment clutter; and $\vec{V}_{tag}^{\,i}$ is the voltage due to the backscatter from the tag when the tag IC (chip) is in state *i*.

These components can be assumed stationary during single tag interrogation. For example, if the reader reads 1000 tags/s and the tag moves at 36 km/h (10 m/s), then during 1 ms that it takes to read the tag, the tag moves only by 1 cm which does not significantly affect propagation channel properties. All three components and their sources are shown in Fig. 1 and 2.

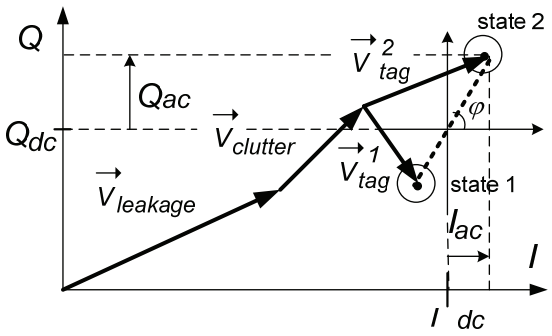

Fig. 1. Complex demodulated voltage received by the reader.

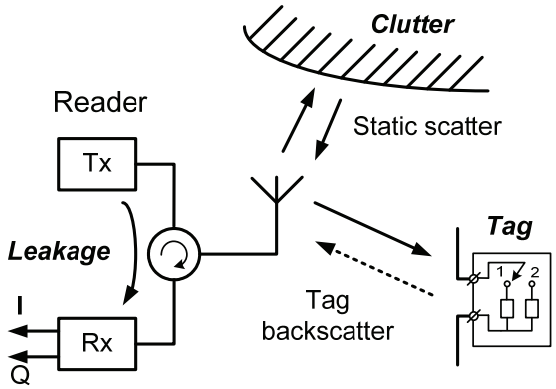

Fig. 2. Sources contributing to the complex demodulated voltage received by the monostatic reader: leakage, clutter, and tag.

At the reader, the in-phase (I) and quadrature (Q) components of the received and demodulated tag signal are composed of DC and AC parts, as shown in Fig. 1:

$$I = I_{dc} + I_{ac} \quad , \quad Q = Q_{dc} + Q_{ac} \,. \tag{2}$$

The DC parts are due (in the diminishing order of importance) to the reader transmit–receive leakage, static environment clutter, and backscatter from the tag (which contains both static and modulated components). The reference point commonly used by readers is mid-point between tag constellation points (states 1 and 2 in Fig. 1).

After the DC part is filtered out, the tag constellation is centered at zero and one can measure both RSSI and phase of the received tag signal as:

$$RSSI = \frac{1}{2}\frac{\left|\vec{V}_{tag}^{\,2} - \vec{V}_{tag}^{\,1}\right|^2}{Z_o} = \frac{I_{ac}^2 + Q_{ac}^2}{Z_o}, \tag{3}$$

$$\varphi = ang\left(\vec{V}_{tag}^{\,2} - \vec{V}_{tag}^{\,1}\right) = arctan\frac{Q_{ac}}{I_{ac}} \tag{4}$$

where Z_0 is the input impedance of the receiver (50 Ω).

For illustration, a typical tag signal seen at the reader (after the DC part removal) is shown in Fig. 3, both in IQ plane (tag signal constellation) and in time domain.

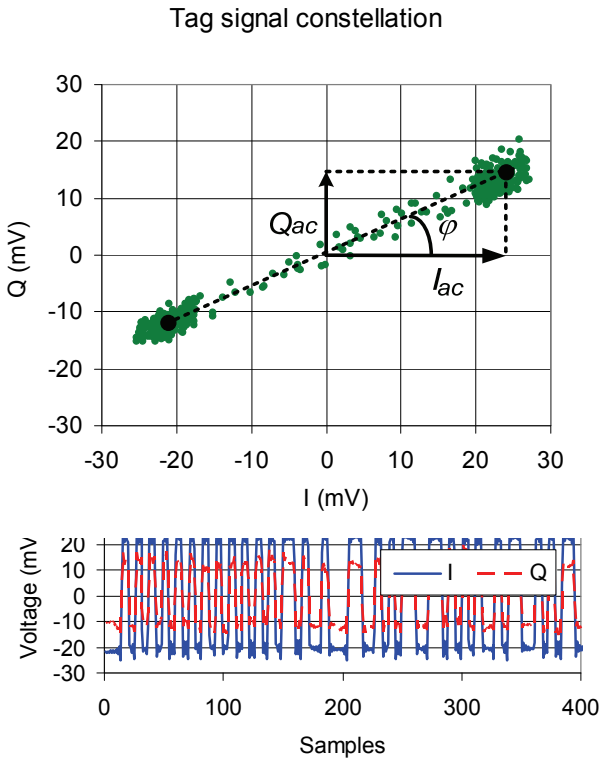

Fig. 3. Typical tag signal received at the reader.

In any propagation environment, the phase of the received tag signal can be written as:

$$\varphi = \varphi_{prop} + \varphi_o + \varphi_{BS}\,, \tag{5}$$

where φ_{prop} is the phase accumulated due to the electromagnetic wave propagation, φ_o is the phase offset which includes phases of the cables and other reader and antenna components, and φ_{BS} is the backscatter phase of the tag modulation.

In free space, using classical phasor formula for electromagnetic field propagating in free space (whose phase is proportional to the distance travelled), one can write:

$$\varphi_{prop} = -2kd \quad , \tag{6}$$

where $k = 2\pi f / c$ is the wavevector (proportional to the frequency) and d is the distance to the tag, One can see that the phase given by equation 6 linearly varies with the distance to the tag. When the tag is moved away or towards the reader (in free space), both vectors $\vec{V}_{tag}^{\,1}$ and $\vec{V}_{tag}^{\,2}$ rotate simultaneously, making full rotation and causing 360 degrees tag signal phase change for every $\lambda / 2$ of radial tag movement.

III. TECHNIQUES

A. TD-PDOA (Time Domain Phase Difference of Arrival)

TD-PDOA allows one to estimate the projection of the tag velocity vector on to the line of sight between the tag and the reader by measuring tag phases at different time moments. It can be viewed as a form of measuring Doppler shift to determine the speed of the mobile node [22-24]. The technique is illustrated in Fig. 4, where the tag moves with a constant speed some distance away from the reader antenna.

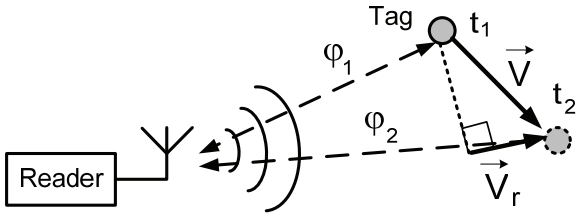

Fig. 4. TD-PDOA illustration.

By measuring the phase of the tag signal at two different time moments (at the fixed frequency), assuming that other two components of the tag phase (phase offset and tag backscatter phase) do not change, and taking the derivative of the phase with respect to time, we can calculate tag radial velocity projection as:

$$V_r = -\frac{c}{4\pi f}\frac{\partial \varphi}{\partial t} \quad . \tag{7}$$

A theoretical application of this technique to RFID recently appeared in [25], where network analyzer was used for channel measurements. Note that the velocity calculated from equation 7 is instantaneous tag velocity, which may change with time (if the tag accelerates/decelerates).

B. FD-PDOA (Frequency. Domain Phase Difference of Arrival)

FD-PDOA allows one to estimate the distance to the tag by measuring tag phase at different frequencies. It can be viewed as a form of ranging using well known frequency modulated continuous wave (FM CW) radar [26-27], or similar harmonic [28-31] radar. The technique is illustrated in Figure 5.

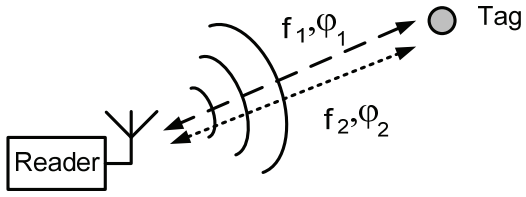

Fig. 5. FD-PDOA illustration.

By measuring the phase of the tag signal at several (two or more) frequencies, taking the derivative of the phase with respect to frequency, and assuming that other two components of the tag phase (phase offset and tag backscatter phase) do not change with frequency or can be calibrated out, and the tag has not moved much (much less than wavelength) during the measurements, we can calculate the range to the tag as:

$$d = -\frac{c}{4\pi}\frac{\partial \varphi}{\partial f} \quad . \tag{8}$$

Note that by using several different reader antennas and applying FD-PDOA to each of them, one can localize the tag in three dimensions, like it is done in FM CW radars [27].Various applications of this technique to RFID in free-space environment recently appeared in [32-38]. Since the FD-PDOA technique is similar to FM CW radar, it can work for both moving and stationary tags.

C. SD-PDOA (Spatial Domain Phase Difference of Arrival)

SD-PDOA allows one to estimate the bearing (direction to the tag), or the angle of arrival, by measuring phases of the tag signal at several receiving antennas. It can be viewed as a form of direction-of-arrival estimation using phased array antenna [39-40]. Many signal processing techniques have been developed in this field to improve angle estimation accuracy [41-42]. The technique is illustrated in Fig. 6 for the bistatic reader configuration (separate transmit and receive antennas).

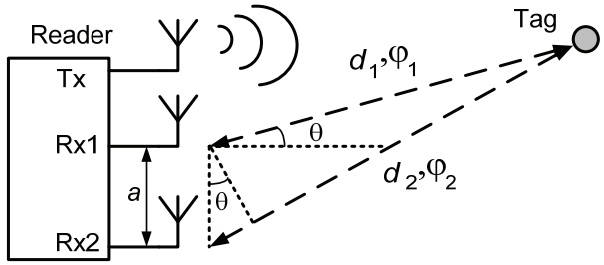

Fig. 6. SD-PDOA illustration.

By measuring the phase difference $\varphi_2 - \varphi_1$ of the received tag signal at two different receiving antennas (at the fixed frequency channel) and attributing it to the path difference $d_2 - d_1$, we can approximately calculate two-dimensional tag bearing as:

$$\theta \approx arcsin\left[-\frac{c}{2\pi f}\frac{(\varphi_2 - \varphi_1)}{a}\right], \tag{9}$$

where a is the spacing between the two receiving antennas. Transmitted antenna can be located anywhere (the phase offset can be calibrated out). Phase measurements on antennas 1 and 2 can either be done simultaneously (in this case, RFID reader needs to have 2-channel receiver) or sequentially (the tag can be interrogated several times, while the receiving antennas are switched between tag queries).

Equation 9 assumes that the tag is far so that simple trigonometry can be used. In general, a set of hyperbolic equations can be used for localization, like it is done in GPS [43]. Note that many variations of SD-PDOA are possible in RFID. For example, an array of several receiving antennas can be used to locate tag in three dimensions [44-45]. Other variations can be found in several issued or pending patents [46-48]. Reader antennas can also be used in monostatic mode (simultaneous transmit/receive). If monostatic configuration is used, equation 9 needs to be modified (the denominator in this case becomes 4π instead of 2π). The bistatic configuration is preferable in SD-PDOA because in all received tag responses, the tag is powered in the same way by separate high gain transmit antenna. Also, receive antennas do not need to have high gain and can be made small and omnidirectional.

IV. MODELING AND SIMULATION EXAMPLE

A. Geometry

Consider the following scenario with the geometry shown in Figure 7. Two reader antennas are mounted at the same height above the ground (shown in yellow color), and the tag is traversing with a constant speed V along the x-axis parallel to the infinite wall (shown in green color). The reader antenna is directional patch and the tag is a dipole oriented along the z-axis (radiation patterns are shown in blue and pink color respectively). The following parameters are used: V=5 mph, b=1.4 m, d=1.3 m, h_{tag} =1.2 m, h_{reader} =1.1 m, a=0.5 m.

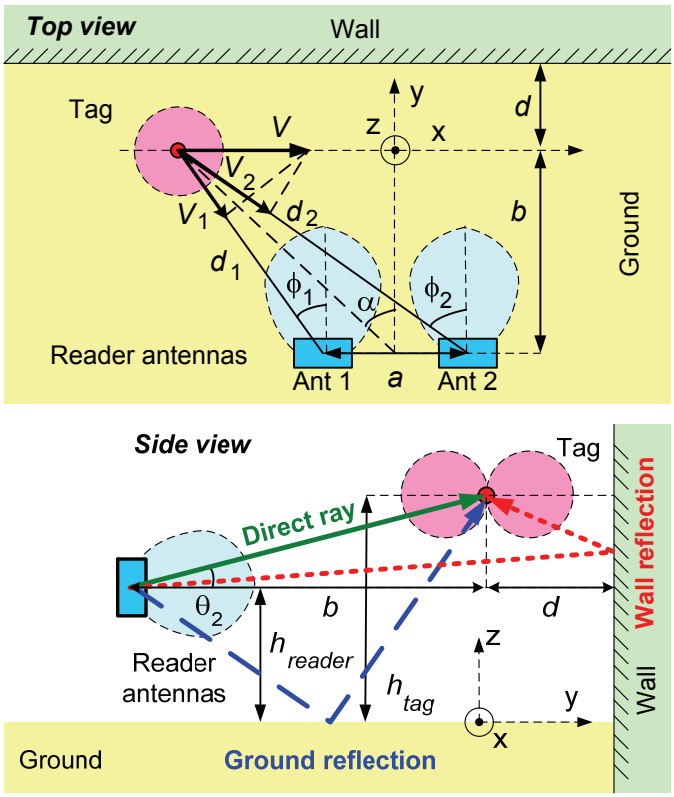

Fig. 7. Geometry of the modeling and simulation example.

B. Channel model

There exist various radio propagation environments. The real propagation environment (the most interesting case) is never free-space. Modeling methods and models for many propagation environments are well known in literature [49-55]. The unique feature of UHF RFID is its short range and the fact that it is based on modulated backscatter. To accurately model RFID channel, both forward and reverse links need to be considered at the same time. Essentially, RFID channel is a double fading channel: each fade is experienced twice, in forward and reverse link [56]. A typical RFID use case scenario involves indoor multipath environment (for example, a warehouse) with the line-of-sight and very few major reflections. Such environment is used in our example. Normally, signal received in wireless environment where the distance to the transmitter is large and there are many independent scatterers can be modeled statistically. However, as mentioned before, passive UHF RFID is a short range technology (even though current passive tags may have range of 50 ft, most practical use case scenarios involve tag reading at 5 to 20 ft distances). While in some cases well known theoretical distributions (Rician, Rayleigh, Nakagami, log-normal) can be used to fit the data [57-59], in general the signal distribution is primarily shaped by the specific geometry and tag trajectories. The multipath in such short range environment is highly deterministic and strongly depends on particular arrangement of nearby reflectors. While numerical 3D EM modeling tools can be applied to such environments and can be especially useful for analyzing complicated cases where various tagged objects are present, such tools normally require significant computation time due to the large problem size relative to the wavelength. Below we describe a deterministic multi-ray model that allows one to calculate the RSSI and phase of the tag signal received at the reader. Because the described model is essentially given by closed-form equations, it can be easily implemented (in Excel or Matlab) and used for system analysis and in RFID network simulators [60].

The path gain of the deterministic multipath channel between the reader and the tag can be written as:

$$G_{path} = \left(\frac{\lambda}{4\pi d_o}\right)^2 |H|^2, \qquad (10)$$

$$H = 1 + \sum_{i=1}^{N} g_t^i g^i \Gamma_i \frac{d_o}{d_i} e^{-jk(d_i - d_o)}, \qquad (11)$$

where d_o is the length of the direct ray path, g_t^i and g^i are the angle-dependent normalized signal gains of the reader and the tag antennas, Γ_i is the angle-dependent reflection coefficient of the i-th reflecting object, d_i is the length of the i-th reflected ray path, and N is the total number of reflections. This multi-ray model is similar to the models described in [61-62] for short range scenarios where other wireless technologies are used for highway applications and where the size of reflectors is large compared to wavelength. The complex factor H can be interpreted as the channel response due solely to multipath. In free space environment, there is no multipath (H=1), and the channel path gain is log-linear, 20 dB/decade. In our example, there are two reflections: from the wall and from the ground. The power of the tag signal received by the monostatic reader can be written as:

$$RSSI = P_t G_t^2 G_{path}^2 K. \qquad (12)$$

where P_t is the output power of the reader, G_t is the gain of the monostatic reader antenna and K is the tag backscatter gain (correspondingly, -K is the tag backscatter loss) which defines how much of the incident RF power is converted to the backscattered modulated power. The phase of the tag signal received at the reader is given by equation 5 where the phase due to the roundtrip propagation channel can be written as:

$$\varphi_{prop} = -2kd_o + 2\arg(H). \qquad (13)$$

To make the problem tractable, we make several simplifying assumptions listed below. Both ground and wall are modeled as flat sheets of perfect conductors (the general expressions of angle-dependent reflection coefficients for non-ideal conductors are well known and can be found for example in [55]). Only single reflections from either reflector (the ground or the wall) are considered. The vertically oriented tag antenna is assumed to have the radiation pattern of an ideal half-wavelength dipole with 2 dBi gain, approximated based on well known angle-dependent expression [63] as:

$$g(\theta,\phi) = \sin^3\theta, \qquad (14)$$

where θ is the angle in the vertical plane (see Fig. 7, side view). The normalized angle-dependent reader antenna pattern in both vertical and horizontal planes iss approximated with the analytical function based on antenna half-power beamwidths:

$$g_r(\theta,\phi) = \cos\left[\frac{\pi}{2}\sin\left(\frac{\pi}{6}\frac{\theta}{\theta_{3dB}}\right)\right]\cos\left[\frac{\pi}{2}\sin\left(\frac{\pi}{6}\frac{\phi}{\phi_{3dB}}\right)\right]. \qquad (15)$$

where φ is the angle in the horizontal plane (see Fig. 7, top view). We assume for simplicity that the phase patterns of both tag and reader antennas are isotropic (independent of angle). Both horizontal and vertical beamwidths of the circularly polarized reader antenna are 60 degrees, and the horizontal and vertical linear gains are 6 dBil. The tag sensitivity is -12 dBm, and the tag backscatter loss (at threshold) is 10 dB, increasing linearly (1 dB/dB) with increasing incident power. The tag backscatter phase is assumed constant (independent of power). These assumptions are based on measurements described in the next section. The reference point is chosen so that $\varphi_{BS} + \varphi_o = 0$. The reader output power is 30 dBm and the frequency is 915 MHz. For every tag position, the paths and angles of three rays: direct, ground reflection, and wall reflection are computed and used in equations 10 and 11 to calculate the RSSI and the phase of the tag at the reader receiver using equations 12 and 13. The model was experimentally verified and agreed well with the data (tag RSSI and phase) collected in the portal environment.

C. *Results*

Figures 8 and 9 show the RSSI and the phase of the tag signal which would be measured at the receiving antenna 2 at 915 MHz as functions of tag position along the x-axis. On antenna 1, one would see the same curves but shifted by 0.5 m (antenna 1 is to the left of antenna 2). One can see that in this example where directional antennas are used, the reflection from the ground is small, and the reflection that influences the RSSI of the tag the most is coming from the wall. Figures 10, 11, and 12 give the tag radial speed projection *V2*, the range to the tag *d2* (using two frequencies, 914 MHz and 915 MHz), and the bearing to the tag α, all obtained from the tag phase using three PDOA techniques described above (TD, FD, and SD).

One can see that the multipath has very strong effect on the tag speed, range, and bearing calculated with PDOA. The most robust technique is TD-PDOA, which even in the presence of multipath allows one to find the direction of the tag movement (ingress/egress) and the center crossing (when the tag passes by the reader).

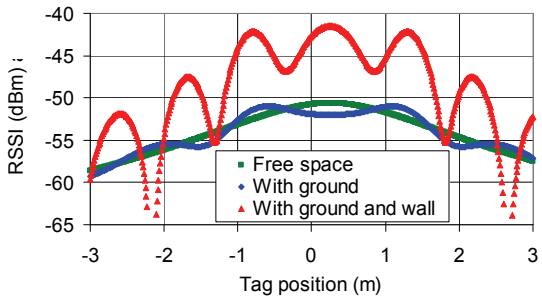

Fig. 8. RSSI of the tag signal received on antenna 2 at 915 MHz

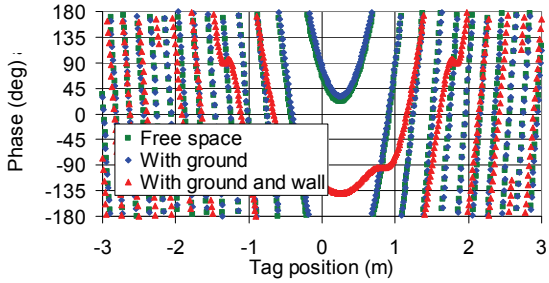

Fig. 9. Phase of the tag signal received on antenna 2 at 915 MHz.

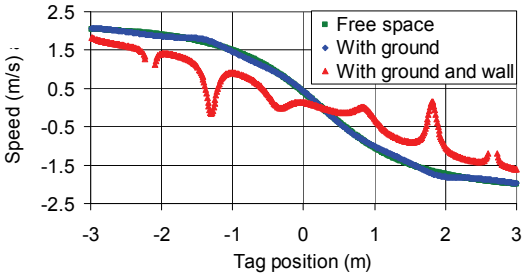

Fig. 10. Tag radial speed relative to ant. 2 obtained with TD-PDOA.

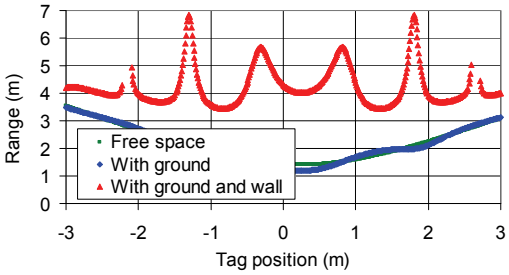

Fig. 11. Range to the tag from ant. 2, obtained with FD-PDOA.

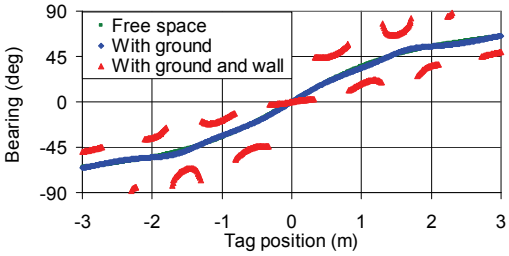

Fig. 12. Bearing to the tag α obtained with SD-PDOA.

V. EXPERIMENTS

Experiments on using phase based techniques to determine tag range, etc. in free space environment have been described by various researchers (see e.g. [36]). In this paper, we would like to discuss the real challenging RFID environment with strong multipath. To illustrate one of the aforementioned approaches (TD-PDOA) in such practical scenario, we performed tag RSSI and phase measurements in a standard warehouse portal (a gate through which tagged goods travel and which is equipped with antennas connected to RFID reader). The tag RSSI and phase characteristics in the portal strongly depend on the geometry of the portal and its antennas, the characteristics of the tags, their relative arrangement and trajectories, the type of tagged goods, etc. This is a good example of challenging RFID environment. Tag RSSI in portal has recently been analyzed in [64] using battery-assisted tag device which recorded signal strength. In our measurements, we used our own custom reader hardware which was capable of accurately measuring both RSSI and phase of the received tag signal. Below, we concentrate on time domain phase measurements to show how TD-PDOA can be utilized in practice.

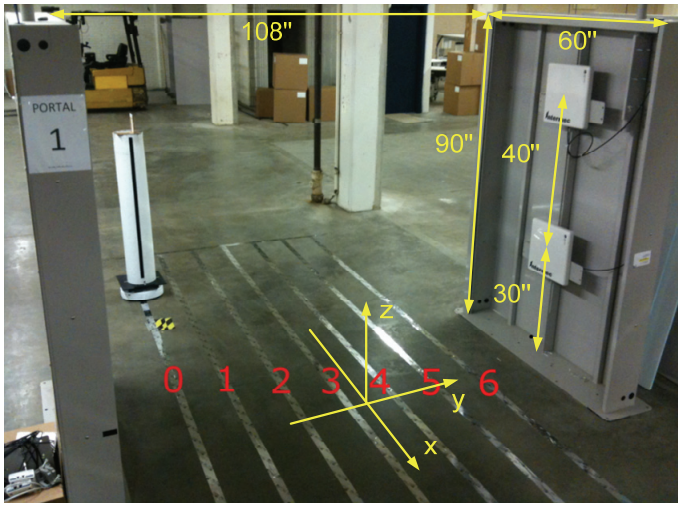

Fig. 13. Experimental RFID portal.

We performed our measurements in the experimental warehouse portal photographed in Figure 13, with the dimensions and the coordinate system as shown. Four antennas were connected to one monostatic RFID reader with four sequentially switched antenna ports. A remote controlled robot carried the styrofoam column with a cardboard piece and RFID tags attached and moved along one of the lines 0-6 (along x-axis), traversing the portal and periodically stopping to allow the reader to take measurements of the RSSI and phase of the received tag signal on all frequency channels in FCC ISM band (902-928 MHz) from all four antennas. The reader transmit power was constant (30 dBm). A large number of tag RSSI and phase data was collected (6 lanes, 4 reader antennas, >20 tags, >200 robot steps, >50 frequency channels).

The portal was made of metal, and the warehouse floor was re-barred concrete. The tags were Avery Dennison dipole-like AD-222 Gen2 tags [65], with Impinj Monza 2 chip. The tags were mounted both horizontally and vertically. The reader antennas were circularly polarized Huber & Suhner RFID antennas (model number SPA 915/60/10/0/RCP [66]), with the maximum gain 10 dBi, axial ratio 2.5 dB, horizontal and vertical beamwidths 45 and 60 degrees (the antennas were rotated 90 degrees to minimize coverage outside the portal).

Because the tag received different power at different points inside portal volume, we needed to know how tag backscatter phase behaved as a function of incident power. We measured it separately, with the variable attenuator connected to the monostatic reader output and the tag placed (first as is, then on cardboard) in anechoic chamber at the distance of d=3 ft from the transmitting antenna (which was linearly polarized, with 6 dBi gain) as shown in Fig. 14. The reader power was constant (30 dBm), and the attenuator allowed to change the output power in 1 dB steps. The phase offset due to the attenuator was separately measured at each attenuation level with the network analyzer and taken into account in measurements.

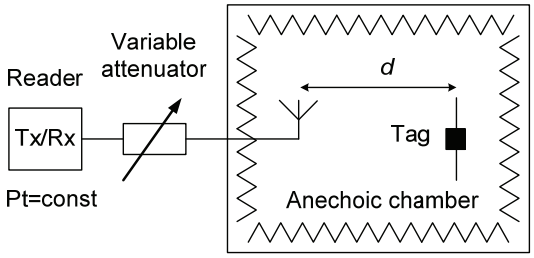

Fig. 14. Experimental setup for tag backscatter characterization.

Figure 15 shows the measured backscatter gain and the backscatter phase as functions of power incident on the tag. Note that since only the relative phase change is important, any reference point can be chosen. We chose the reference point so that the tag phase is zero at threshold power when the tag is measured as is. The measured threshold backscatter loss for the AD-222 tag on cardboard (when incident power was equal to threshold tag sensitivity) was about -10 dB. Measurements in Figure 15 are given for one frequency, 915 MHz. Measurements at other frequencies showed similar results and confirmed that the tag phase variation due to the varying power of the incident signal (less than ten degrees) is small compared to phase changes due to tag motion (several hundred degrees).

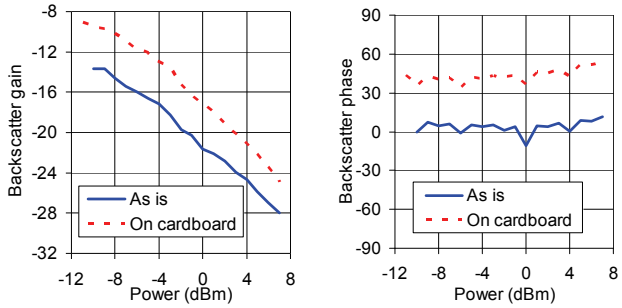

Fig. 15. Backscatter gain and phase as functions of power incident on the tag at 915 MHz in free space (as is and on cardboard).

We performed measurements for all tags traversing our portal at different heights at all six lanes. A typical measured tag phase when the tag traverses through our portal is shown in Fig. 16 for the case when the tag is at z=0.93 m above the ground, it travels on lane 3 (y=-0.1 m) and the signal is received on one of the lower reader antennas (y=-1.45 m) at 902 MHz. For some tag positions (when tag enters/leaves portal), the tag was not powered up, and hence the phase value was not available as can be seen from Fig. 17.

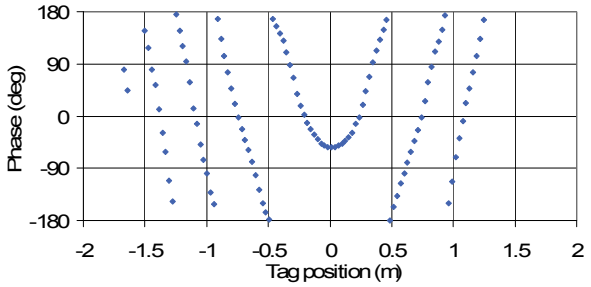

Fig. 16. Measured phase of the tag traversing through the portal.

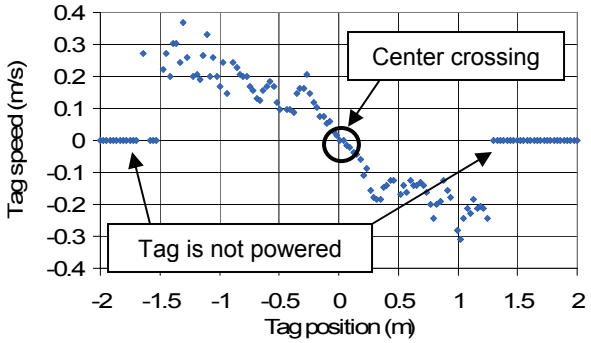

Fig. 17. Radial speed of the tag traversing the portal: calculated from data with TD-PDOA and the actual (zero speed means tag is not read).

An application of TD-PDOA technique to the measured phase data is shown in Fig. 17 and allows one to calculate the radial speed projection of the tag. As one can see, the ingress/egress direction of the tag movement (radial speed positive or negative) and the point when the tag crosses the center (radial speed is zero) can easily be identified.

The FD-PDOA experimental results with the portal were similar to the results presented in Fig. 11 for the modeling and simulation example: the multipath had very strong effect on ranging with FD-PDOA. As for SD-PDOA, our experimental data was not well suited to apply this technique because the four-antenna reader was monostatic and the pairs of antennas mounted on each side of standard portal were arranged vertically instead of horizontally.

We have also performed a series of experiments in anechoic chamber where we observed that both FD-PDOA and SD-PDOA can work really well for UHF RFID in the absence of reflections. Similar results have been noticed by other researchers (see e.g. [36]).

VI. CONCLUSIONS

In this paper, we gave an overview of phase based spatial identification of modulated backscatter tags. We described three main approaches (TD-PDOA, FD-PDOA, and SD-PDOA), presented a modeling and simulation example and analyzed experimental data collected in real multipath RFID scenario: a warehouse portal. We also described the deterministic multipath channel model for UHF RFID systems which was used in our simulations.

It was observed both in simulations and in experiments that TD-PDOA technique was fairly robust to multipath. The ingress/egress direction of the tag movement (radial speed positive or negative) and the point when the tag crosses the center (radial speed is zero) could easily be identified.

The real challenge is to make both FD-PDOA and SD-PDOA techniques work reliably in an arbitrary environment, where location of short range multipath sources is unknown. The fact that the available bandwidth is small (<30 MHz in UHF ISM band) makes this problem especially difficult. This is a subject of current and future research.

REFERENCES

[1] H. Liu et al., "Survey of Wireless Indoor Positioning Techniques and Systems", IEEE Transactions on Systems, Man, and Cybernetics, vol. 37, no. 6, Nov. 2007, pp. 1067 - 1080

[2] M. Vossiek et al., "Wireless local positioning", IEEE Microwave Magazine, vol. 4, Issue 4, Dec. 2003, pp. 77 – 86

[3] G. Yanying, A. Lo, L. Niemegeers, "A survey of indoor positioning systems for wireless personal networks", IEEE Communications Surveys & Tutorials, vol. 11, no. 1, 2009, pp. 13 – 32

[4] P. Gulden, S. Roehr, M. Christmann, "An overview of wireless local positioning system configurations", IEEE Int. Microwave Workshop on Wireless Sensing, Local Positioning, and RFID, Sept. 2009, pp. 1 – 4

[5] K. Pahlavan, L. Xinrong J. P. Makela, "Indoor geolocation science and technology", IEEE Communications Magazine, vol. 40, no. 2, Feb. 2002, pp. 112 - 118

[6] H. Schau, A. Robinson, "Passive source localization employing intersecting spherical surfaces from time-of-arrival differences", IEEE Transactions on Acoustics, Speech and Signal Processing, vol. 35, no. 8, Aug 1987, pp. 1223 – 1225

[7] K. Frampton, "Acoustic self-localization in a distributed sensor network", IEEE Sensors Journal, vol. 6, no. 1, Feb. 2006, pp. 166 – 172

[8] B. Friedlander, "A Passive Localization Algorithm and Its Accurancy Analysis", IEEE Journal of Oceanic Engineering, vol. 12, no. 1, Jan 1987, pp. 234 – 245

[9] J. Smith, J. Abel, "The spherical interpolation method of source localization", IEEE Journal of Oceanic Engineering, vol. 12, no. 1, Jan 1987, pp. 246 – 252

[10] M. Fowler, H. Xi, "Signal models for TDOA/FDOA estimation", IEEE Transactions on Aerospace and Electronic Systems, vol. 44, no. 4, Oct. 2008, pp. 1543 – 1550

[11] M. Bouet, A. L. dos Santos, "RFID tags: Positioning principles and localization techniques", 1st IFIP Wireless Days, Nov. 2008, pp.1 – 5

[12] J. Zhou, J. Shi, "RFID localization algorithms and applications—a review", Journal of Intelligent Manufacturing, vol. 20, no. 6, December, 2009, pp. 695-707

[13] C. Yu, R. Liu, "Application of RF Tags in Highway Reference Markers", International IEEE Conference on Intelligent Transportation Systems, Oct. 2008, pp. 464 – 469

[14] Youngsu Park et al., "Improving position estimation on RFID tag floor localization using RFID reader transmission power control", IEEE Int. Conference on Robotics and Biometrics, Feb. 2009, pp. 1716 - 1721

[15] E. Bruns et al., "Enabling Mobile Phones To Support Large-Scale Museum Guidance", IEEE Multimedia, vol. 14, no. 2, April-June 2007, pp. 16 - 25

[16] A. Reza, T. Geok, "Investigation of Indoor Location Sensing via RFID Reader Network Utilizing Grid Covering Algorithm", Wireless Personal Communications, vool. 49, no. 1, April 2009, pp. 67-80

[17] A. Chattopadhyay, A.Harish, "Analysis of low range Indoor Location Tracking techniques using Passive UHF RFID tags", IEEE Radio and Wireless Symposium, Jan. 2008, pp. 351 – 354

[18] C. Alippi et al., "A statistical approach to localize passive RFIDs", IEEE Int. Symposium on Circuits and Systems, pp. 843-846

[19] M. Kim, N. Chong, "Direction Sensing RFID Reader for Mobile Robot Navigation", IEEE Transactions on Automation Science and Engineering, vol. 6, no. 1, Jan. 2009, pp. 44 - 54

[20] Y. Oikawa, "Tag movement direction estimation methods in an RFID gate system", 6th International Symposium on Wireless Communication Systems, 7-Sept. 2009, pp. 41 – 45

[21] T. Hansen, M. Oristaglio, "Method for Controlling the Angular Extent of Interrogation Zones in RFID", IEEE Antennas and Wireless Propagation Letters, vol. 5, no. 1, Dec. 2006, pp. 134 – 137

[22] B. Kusy et al., "Tracking Mobile Nodes Using RF Doppler Shifts", ACM Conf. on Embedded Networked Sensor Syst., Nov. 2007, pp. 1-14

[23] H. Jingyu et al., "The phase probability distribution of general Clarke model and its application in Doppler shift estimator", IEEE Antennas and Wireless Propagation Letters, vol. 4, 2005, pp. 373 – 377

[24] C. Xiao, K. Mann, J. Olivier, "Mobile speed estimation for TDMA-based hierarchical cellular systems" IEEE Transactions on Vehicular Technology, vol. 50, no. 4, July 2001, pp. 981 - 991

[25] B. Yanakiev et al., "Assessment of the Physical Interface of UHF Passive Tags for Localization", 1st International EURASIP Workshop on RFID, Sept. 2007, pp. 1-4

[26] H. Griffiths, "New ideas in FM radar", Electronics & Communication Engineering Journal, vol. 2, no. 5, Oct. 1990, pp. 185 - 194

[27] M.Vossiek at al., "Inverse Synthetic Aperture Secondary Radar Concept for Precise Wireless Positioning", IEEE Transactions on Microwave Theory and Techniques, vol. 55, no. 11, Nov. 2007, pp. 2447 – 2453

[28] J. Shefer, R. Klensch, "Harmonic radar helps autos avoid collisions", IEEE Spectrum, vol. 10, no. 5, May 1973, pp. 38 – 45

[29] B. Colpitts, G. Boiteau, "Harmonic radar transceiver design: miniature tags for insect tracking", IEEE Transactions on Antennas and Propagation, vol. 52, no. 11, Nov. 2004, pp. 2825 – 2832

[30] D. Psychoudakis et al., "A Portable Low-Power Harmonic Radar System and Conformal Tag for Insect Tracking", IEEE Antennas and Wireless Propagation Letters, vol. 7, 2008, pp. 444 - 447

[31] E. de Moura Presa, et al., "A new microwave harmonic direction-finding system for localization of small mobile targets using passive tags", Microw. and Opt. Techn. Letters, vol. 47, no. 2, Oct. 2005, pp. 134-137

[32] S. Kunkel et al., "A concept for infrastructure independent localization and augmented reality visualization of RFID tags", IEEE Int. Microwave Workshop on Wireless Sen., Local Pos., and RFID, Sept. 2009, pp. 1 – 4

[33] J. Heidrich et al., "Local positioning with passive UHF RFID transponders", IEEE Int. Microwave Workshop on Wireless Sensing, Local Positioning, and RFID, Sept. 2009, pp. 1 – 4

[34] X. Li, Y. Zhang; M. Amin, "Multifrequency-based range estimation of RFID Tags", IEEE RFID Conference, April 2009, pp. 147 - 154

[35] Y. Zhang, X. Li, and M. G. Amin, "Array processing for RFID tag localization exploiting multi-frequency signals", SPIE Defense, Security, and Sensing Symposium, April 2009

[36] D. Arnitz, K. Witrisal, U. Muehlmann, "Multifrequency Continuous-Wave Radar Approach to Ranging in Passive UHF RFID", IEEE Transactions on MTT, , vol. 57, no. 5, May 2009 , pp. 1398 – 1405

[37] T. Ussmueller, M. Jung, R. Weigel, "Synthesizer concepts for FMCW based locatable wireless sensor nodes", IEEE Int. Microwave Workshop on Wireless Sensing, Local Positioning, and RFID, Sept. 2009, pp. 1 – 4

[38] P. Hoogeboom, F. Elferink, C. Trampuz, "Development of a switching passive 2.4 GHz RFID transponder on flexible substrate", European Microwave Conference, Sept.-Oct. 2009, pp. 165 - 168

[39] W. Von Aulock, "Properties of Phased Arrays", Proceedings of the IRE, vol. 48, no. 10, Oct. 1960, pp. 1715 - 1727

[40] L. Brennan, "Angular accuracy of a phased array radar", IRE Trans. on Antennas and Propagation, vol. 9, no. 3, May 1961, pp. 268 – 275

[41] J. Fuhl, J.-P. Rossi, E. Bonek, "High-resolution 3-D direction-of-arrival determination for urban mobile radio", IEEE Transactions on Antennas and Propagation, vol. 45, no. 4, April 1997, pp. 672 – 682

[42] H. Gazzah, K. Abed-Meraim, "Optimum Ambiguity-Free Directional and Omnidirectional Planar Antenna Arrays for DOA Estimation", IEEE Trans. on Signal Processing, vol. 57, no. 10, Oct. 2009, pp. 3942-3953

[43] J. Chaffee, J.Abel, "On the exact solutions of pseudorange equations", IEEE Transactions on Aerospace and Electronic Systems, vol. 30, no. 4, Oct. 1994, pp. 1021 - 1030

[44] Y. Zhang, M. Amin, S. Kaushik, "Localization and Tracking of Passive RFID Tags Based on Direction Estimation", International Journal of Antennas and Propagation, October 2007, pp. 1-9

[45] J. Wang, M. Amin, Y. Zhang, "Signal and array processing techniques for RFID readers", Proceedings of the SPIE, volume 6248, 2006

[46] "Method and apparatus to determine the direction to a transponder in a modulated backscatter system", US Patent 6476756

[47] "Utilization of motion and spatial identification in mobile RFID interrogator", US patent application 20090207024

[48] "Method and System to Determine the Orientation, Size, Position, and Movement of RFID Tagged Objects", US patent application 12/495,732

[49] T. S. Rappaport, "Characterization of UHF multipath radio channels in factory buildings", IEEE Transactions on Antennas and Propagation, vol. 37, no. 8, Aug. 1989, pp. 1058 – 1069

[50] H. Hashemi, "The indoor radio propagation channel", Proceedings of the IEEE, vol. 81, no. 7, July 1993, pp. 943 - 968

[51] H. Bertoni, W. Honcharenko, L. Macel, H. Xia, "UHF propagation prediction for wireless personal communications", Proceedings of the IEEE, vol. 82, no. 9, Sept. 1994, pp. 1333 – 1359

[52] T. K.Sarkar, J. Zhong, K. Kim, A. Medouri, M. Salazar-Palma, "A survey of various propagation models for mobile communication", IEEE Antennas and Propagation Magazine, June 2003, vol. 45, pp. 51-82

[53] C. H. Bianchi and K. Sivaprasad, "A channel model for multipath interference on terrestrial line-of-sight digital radio", IEEE Transactions on Antennas and Propagation, vol. 46, no. 6, June 1998, pp. 891 – 901

[54] A. Neskovic, N. Neskovic, G. Paunovic, "Modern approaches in modeling of mobile radio systems propagation environment", IEEE Comm. Surveys and Tutorials, vol. 3, no. 3, 2000, pp. 2 - 12

[55] H. Xia, H. Bertoni, L. Maciel, A. Lindsay-Stewart, R. Rowe, "Radio propagation characteristics for line-of-sight microcellular and personal communications", IEEE Transactions on Antennas and Propagation, vol. 41, no. 10, Oct. 1993, pp. 1439 - 1447

[56] J. Griffin, G. Durgin, "Complete Link Budgets for Backscatter-Radio and RFID Systems", IEEE Antennas and Propagation Magazine, vol. 51, no. 2, April 2009, pp. 11 – 25

[57] D. Kim, M. A. Ingram, and W. W. Smith, "Measurements of small-scale fading and path loss for long range RF tags", IEEE Transactions on Antennas and Propagation, vol. 51, no. 8, Nov. 2003, pp. 1740-1749

[58] L. Mayer, M. Wrulich, S. Caban, "Measurements and channel modeling for short range indoor UHF applications", First European Conference on Antennas and Propagation, Nov. 2006, pp. 1 – 5

[59] A. Lazaro, D. Girbau, D. Salinas, "Radio Link Budgets for UHF RFID on Multipath Environments", IEEE Transactions on Antennas and Propagation, vol. 57, no. 4, part 2, April 2009, pp. 1241 – 1251

[60] C. Floerkemeier, S. Sarma, "RFIDSim—A Physical and Logical Layer Simulation Engine for Passive RFID", IEEE Trans. on Automation Science and Engineering, vol. 6, no. 1, Jan. 2009, pp. 33 – 43

[61] A. Domazetovic, L. Greenstein, N. Mandayam, I. Seskar, "Propagation models for short-range wireless channels with predictable path geometries", IEEE Transactions on Communications, vol. 53, no. 7, July 2005, pp. 1123 – 1126

[62] M. Toyota, R. Pokharel, O. Hashimoto, "Efficient multi-ray propagation model for DSRC EM environment on express highway", Electronics Letters, vol. 40, no. 20, Sept. 2004, pp. 1278 – 1279

[63] C. Balanis, "Antenna Theory: Analysis and Design", Wiley, 2005

[64] U. Muehlmann et al., "Modeling and Performance Characterization of UHF RFID Portal Applications", IEEE Transactions on Microwave Theory and Techniques, vol. 57, no. 7, July 2009, pp. 1700 – 1706

[65] Avery Dennison RFID Products [Online]. Available: http://www.rfid.averydennison.com/us/products_portfolio.php

[66] Huber & Suhner RFID antennas, available at: http://www.hubersuhner.com/mozilla/products/hs-p-rf/hs-rf-antennas/hs-p-rf-ant-rfid